Progress In Electromagnetics Research, PIER 44, 81–101, 2004

A TIME DOMAIN INCREMENTAL THEORY OF DIFFRACTION: SCATTERING OF ELECTROMAGNETIC PULSED PLANE WAVES

A. M. Attiya and E. El-Diwany

Department of Microwave Engineering
Electronic Research Institute, Dokki
Giza, 12211, Egypt

A. M. Shaarawi †

The Physics Department
The American University in Cairo
P.O. Box 2511, Cairo 11511, Egypt

I. M. Besieris

The Bradley Department of Electrical and Computer Engineering
Virginia Polytechnic Institute and State University
Blacksburg, Virginia 24061, USA

Abstract—A new formulation of a time domain incremental theory is introduced. This approach is applied to the scattering of a pulsed plane wave incident on a circular disk. It is shown that the scattered field is free from singularities at caustics and exhibits a notable wave structure outside Keller's cone.

† On leave from the Department of Engineering Physics and Mathematics, Faculty of Engineering, Cairo University, Giza 12211, Egypt.

1. INTRODUCTION

In recent years, Tibero et al. [1–4] have developed an effective technique for evaluating the scattering of high-frequency fields. Their technique is known as the incremental theory of diffraction (ITD). The ITD eliminates caustic singularities of ray techniques and at the same time extends the predictions of the scattered fields outside the diffraction cone. In the frequency domain formulation of ITD [2–4], Tibero et al. have demonstrated that the scattered fields calculated using ITD reduce to the ones resulting from applying the uniform theory of diffraction (UTD) [5–7] in the limit when the structure resembles locally an infinite wedge. Thus, one can start by employing the analytical solution of the canonical problem of an infinite wedge in order to determine the incremental diffracted fields due to each point on an infinite edge. Each incremental point on an arbitrary finite wedge can be represented as an incremental point on a local infinite wedge, as shown in Fig. 1. The diffracted field of each incremental point is simply the incremental diffracted field of the canonical problem of the infinite wedge [8–10]. The total diffracted field due to an arbitrary finite edge can be obtained by adding such incremental fields radiated from each point on the edge. One advantage of this approach is that in ITD the

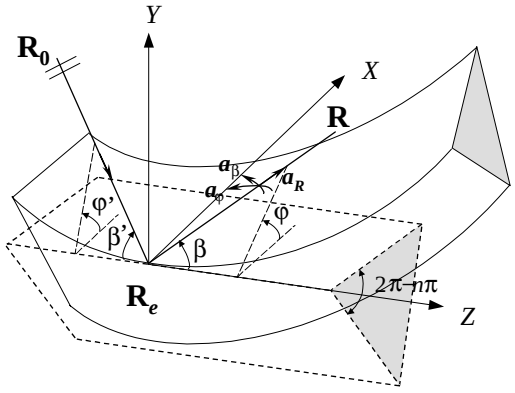

Figure 1. A canonical problem of a locally tangent wedge used for defining incremental diffraction contributions and its relevant geometry.

diffracted fields are obtained directly in terms of the incident fields and not in terms of an equivalent current distribution along the edge [11–13]. On the other hand, the part of the field scattered from the surface of a finite scatterer can be obtained by the physical optics (PO) method [14–17]. This is done by discretizing the surface into small sub-surfaces, the surface current distribution is determined from the incident tangential magnetic field and the scattered field results from integrating contributions from each sub-surface, as shown in Fig. 2. The end-points of the surface at the shadow boundary curve should be treated separately in this case because they represent half-illuminated sub-surfaces, as illustrated in Fig. 3. It should be noted that the shadow boundary line, which represents the end-points of the physical optics part, does not necessarily coincide with an edge line. In fact, the scattering body may have a shadow boundary line but does not have an edge, as illustrated for the ellipsoid shown in Fig. 2.

In a later article, Capolino and Tibero [1] developed a time domain incremental theory of diffraction (TD-ITD). That method was applied to situations involving the diffraction of a band limited scalar field from a circular slit. A recipe was also included to show how the TD-ITD could be extended to the vector electromagnetic case using a dyadic formulation. Unlike the original FD-ITD, Capolino and Tibero used transition functions in their TD-ITD from the geometric theory of diffraction instead of the UTD. The resulting inverse Fourier transform contained a dispersion-free kernel that facilitated their time domain formulation.

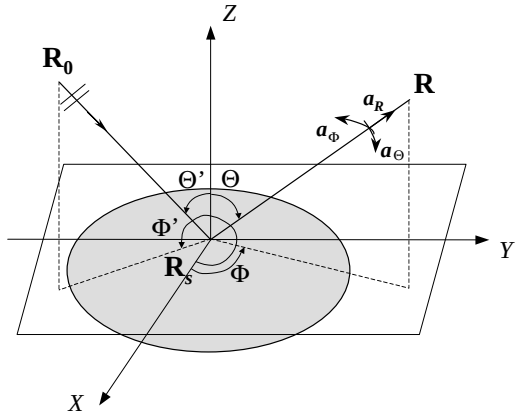

Figure 2. A locally tangent flat plane for defining incremental PO contributions and its relevant geometry.

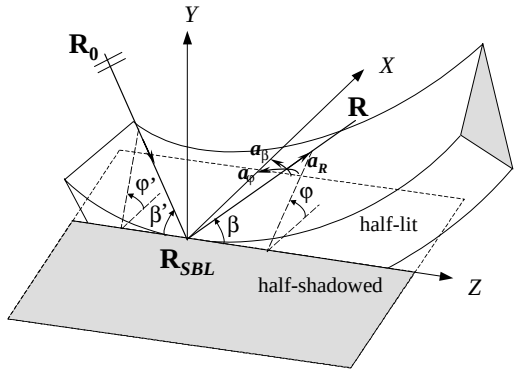

Figure 3. A locally tangent semi-lit flat plane for defining incremental PO end-point contributions and its relevant geometry.

In this paper, we develop a TD-ITD approach that differs from the one adopted by Capolino and Tibero. In particular, we formulate an incremental theory of diffraction based on transition functions derived from the UTD. In addition, we deal directly with the vector case involving the scattering of electromagnetic pulses. The analysis provided in this paper is extended in Ref. [18] to the study of scattering of a transverse electric (TE) ultra-wideband X-wave from a conducting disk.

2. FREQUENCY DOMAIN INCREMENTAL THEORY OF DIFFRACTION

The incremental theory of diffraction is based on dividing the total scattered field into three parts: the physical optics part, the end-point contribution of the shadow-boundary-line and the diffracted field. The physical optics component is given by the surface integration [3]

$$\vec{E}_s^{PO}(\vec{R},\omega) = \iint\limits_S \vec{F}^{PO}\left(\vec{R},\vec{R}_s,\omega\right) dS, \tag{1}$$

where $\vec{F}^{PO}(\vec{R},\vec{R}_s,\omega)$ denotes the physical optics field due an elementary point on the illuminated surface of the scattering object. The position vectors of the various points on the surface are denoted by $\vec{R}_s$. The correction term of physical optics due to the end-points on the shadow-boundary-line can be expressed as the line integration [3]

$$\vec{E}_{SBL}^{PO}(\vec{R},\omega) = \int\limits_{SBL} \vec{F}_{SBL}^{PO}\left(\vec{R},\vec{R}_{SBL},\omega\right) dl, \tag{2}$$

where $\vec{F}_{SBL}^{PO}(\vec{R},\vec{R}_{SBL},\omega)$ denotes an end-point field contribution due to an elementary point $\vec{R}_{SBL}$ on the shadow boundary line (SBL). The generalized geometrical optics part of the scattered field can be expressed as [3]

$$\vec{E}^{go}(\vec{R},\omega) = \vec{E}_s^{PO}(\vec{R},\omega) - \vec{E}_{SBL}^{PO}(\vec{R},\omega). \tag{3}$$

Finally, the diffracted part of the scattered field due to the edge equals [3]

$$\vec{E}^{d}(\vec{R},\omega) = \int\limits_e \vec{F}^{d}\left(\vec{R},\vec{R}_e,\omega\right) dl, \tag{4}$$

where $\vec{F}^{d}(\vec{R},\vec{R}_s,\omega)$ denotes the diffracted field due an elementary point on the local edge of the scattering body. The total scattered field at any observation point in the frequency domain is given by

$$\vec{E}_s^{tot}(\vec{R},\omega) = \vec{E}^{go}(\vec{R},\omega) + \vec{E}^{d}(\vec{R},\omega). \tag{5}$$

To convert this result from the frequency domain to the time domain, one can use a semi-infinite analytic Fourier transformation, viz.,

$$\vec{E}_s^{tot}(\vec{R},t) = \frac{1}{\pi}\mathrm{Re}\left[\int\limits_0^\infty d\omega \exp(j\omega t)\vec{E}_s^{tot}(\vec{R},\omega)\right]. \tag{6}$$

In this work, we convert the aforementioned formulation from the frequency domain to the time domain for a special class of electromagnetic pulsed plane waves; specifically, pulses arising from a Laplace-type spectral superposition. Numerical results, provided in Sec. 4, demonstrate the effectiveness of our time-domain approach in calculating the scattered fields of ultra-short localized pulses from finite scattering structures having curved edges.

3. TIME-DOMAIN FORMULATION OF THE SCATTERING OF AN ELECTROMAGNETIC PULSED PLANE WAVE FROM A PERFECTLY CONDUCTING CIRCULAR DISK

In this section, we use ITD to derive the scattered field in the frequency domain for the case of an electromagnetic pulsed plane wave incident on a perfectly conducting circular disk. Subsequently, the corresponding time domain results are obtained by means of an analytic Fourier transformation. The spectral representation of the incident wave is chosen as an exponentially decaying function of frequency, viz.,

$$\vec{E}_i(\vec{R},\omega) = E_i(\vec{R},\omega)\vec{e}_i = \exp\left(-j\omega\left(\vec{R}-\vec{R}_0\right)\cdot\vec{s}_i/c\right)\exp\left(-\omega a_0/c\right)\vec{e}_i, \tag{7a}$$

which corresponds to an incident pulsed plane wave of the form

$$\vec{E}_i(\vec{R},t) = \mathrm{Re}\left\{\frac{c}{\pi\left(a_0 - j\left(ct - (\vec{R}-\vec{R}_0)\cdot\vec{s}_i\right)\right)}\right\}\vec{e}_i, \tag{7b}$$

where $\vec{e}_i$ is the polarization vector of the incident electric field and $\vec{s}_i$ is the direction of wave propagation. The advantage of the exponentially decaying spectral function given in Eq. (7a) is that it yields a closed form expression when the analytic inverse Fourier transformation is evaluated.

3.1. The Physical Optics Term

The physical optics part of the scattered field, given in Eq. (1), can be calculated as an integration of the elementary amplitude $\vec{F}^{PO}(\vec{R},\vec{R}_s,\omega)$ over the surface of the scatterer. The vector $\vec{R}_s = x_s\vec{a}_x + y_s\vec{a}_y + z_s\vec{a}_z$ is the position of an elementary scattering point on the surface of the scattering body and $\vec{R} = x\vec{a}_x + y\vec{a}_y + z\vec{a}_z$ is the observation point. The physical optics elementary amplitude is given

explicitly as [3],

$$\vec{F}^{PO}(\vec{R},\vec{R}_s,\omega) = \frac{-2\mathrm{U}((\pi/2)-\Theta')}{4\pi|\vec{R}-\vec{R}_s|}\left(\vec{\vec{S}}_s^{PO}(\vec{R}_s)\cdot\vec{e}_i\right) j(\omega/c) \exp\left(-j(\omega/c)|\vec{R}-\vec{R}_s|\right) E_i(\vec{R}_s,\omega). \quad (8a)$$

Here, $\mathrm{U}(\cdot)$ is the unit-step function and $\vec{\vec{S}}_s^{PO}(\vec{R}_s)$ is the scattering dyadic expressed in the local scattering spherical coordinates as follows [3]:

$$\begin{aligned}\vec{\vec{S}}_s^{PO}(\vec{R}_s) \;=\; & \cos\Theta\cos(\Phi-\Phi')\vec{a}_\Theta\vec{a}_{\Theta'} + \cos\Theta\cos\Theta'\sin(\Phi-\Phi')\vec{a}_\Theta\vec{a}_{\Phi'} \\ & -\sin(\Phi-\Phi')\vec{a}_\Phi\vec{a}_{\Theta'} + \cos\Theta'\cos(\Phi-\Phi')\vec{a}_\Phi\vec{a}_{\Phi'}. \quad (8b)\end{aligned}$$

The spherical variables (Θ',Φ') and (Θ,Φ) indicate the directions of the incident and scattered waves in the local scattering coordinates, as shown in Fig. 2. These local spherical coordinates are defined so that the local Z direction is the normal to the surface of the scattering body at the scattering point. The tangential plane at the scattering point contains the local X and Y directions. The local coordinate directions and their relationship to the general Cartesian coordinate system are provided in Appendix A for the specific case of a disk-shaped scatterer. Furthermore, details of the explicit evaluation of the Cartesian coordinates of the field scattered from a circular disk are presented in the same appendix.

3.2. The Diffracted and the Physical Optics Shadow-Boundary-Line Terms

The shadow-boundary-line field of the physical optics part and the diffracted field due to the edge have several characteristics in common. Consequently, the expressions for these two parts are presented together in this subsection. The frequency domain amplitudes of these two parts can be written as [3]

$$\begin{aligned}\vec{F}_{SBL}^{PO}(\vec{R},\vec{R}_{SBL},\omega) \;=\; & \vec{\vec{S}}_{SBL}^{PO}(\vec{R},\vec{R}_{SBL},\omega)\cdot\vec{e}_i E_i(\vec{R}_{SBL},\omega) \\ & \cdot\frac{\exp\left(-j(\omega/c)|\vec{R}-\vec{R}_{SBL}|\right)}{2\pi|\vec{R}-\vec{R}_{SBL}|}, \quad (9a)\end{aligned}$$

and

$$\vec{F}^{d}(\vec{R},\vec{R}_e,\omega) = \vec{\vec{S}}^{\,d}(\vec{R},\vec{R}_e,\omega)\cdot\vec{e}_i E_i(\vec{R}_e,\omega)\frac{\exp\left(-j(\omega/c)|\vec{R}-\vec{R}_e|\right)}{2\pi|\vec{R}-\vec{R}_e|}. \quad (9b)$$

The shadow-boundary line and the edge diffraction function dyadics $\vec{\vec{S}}^{PO}_{SBL}(\vec{R},\vec{R}_{SBL},\omega)$ and $\vec{\vec{S}}^{d}(\vec{R},\vec{R}_{e},\omega)$ are given by

$$\vec{\vec{S}}^{PO}_{SBL}(\vec{R},\vec{R}_{SBL},\omega)=S^{PO}_{\beta\beta'}\vec{a}_{\beta}\vec{a}_{\beta'}+S^{PO}_{\beta\phi'}\vec{a}_{\beta}\vec{a}_{\varphi'}+S^{PO}_{\varphi\beta'}\vec{a}_{\varphi}\vec{a}_{\beta'}+S^{PO}_{\varphi\varphi'}\vec{a}_{\varphi}\vec{a}_{\varphi'}, \tag{10a}$$

and

$$\vec{\vec{S}}^{d}(\vec{R},\vec{R}_{e},\omega)=S^{d}_{\beta\beta'}\vec{a}_{\beta}\vec{a}_{\beta'}+S^{d}_{\beta\varphi'}\vec{a}_{\beta}\vec{a}_{\varphi'}+S^{d}_{\varphi\beta'}\vec{a}_{\varphi}\vec{a}_{\beta'}+S^{d}_{\varphi\varphi'}\vec{a}_{\varphi}\vec{a}_{\varphi'}, \tag{10b}$$

where the directions $\vec{a}_{\beta}$ and $\vec{a}_{\varphi}$ for the cases of the local wedge and the local semi-lit half planes are illustrated in Figs. 1 and 3. The details of the evaluation of $\vec{\vec{S}}^{PO}_{SBL}(\vec{R}_{SBL})\cdot\vec{e}_i$ and $\vec{\vec{S}}^{d}(\vec{R}_e)\cdot\vec{e}_i$ are presented in Appendix B, together with the necessary calculations needed to transform from the local to the general coordinate system and vise versa. The elements of the shadow boundary dyadic are equal to [3]

$$\begin{aligned} S^{PO}_{\beta\beta'}(\varphi,\varphi',\beta;\omega) &= \frac{\sqrt{j(\omega/c)}}{2}\sum_{\ell=1}^{2}F\left((\omega/c)|\vec{R}-\vec{R}_{SBL}|\sin^2\beta b_{\ell}(\varphi,\varphi')\right) \\ &\quad\cdot L^{E}_{\ell}\mathrm{U}(\pi-\varphi'), \qquad (11a)\\ S^{PO}_{\beta\varphi'} &= -\mathrm{U}(\pi-\varphi')\cos\beta, \qquad (11b)\\ S^{PO}_{\varphi\beta'} &= 0, \qquad (11c)\\ S^{PO}_{\varphi\varphi'}(\varphi,\varphi',\beta;\omega) &= \frac{\sqrt{j(\omega/c)}}{2}\sum_{\ell=1}^{2}F\left((\omega/c)|\vec{R}-\vec{R}_{SBL}|\sin^2\beta b_{\ell}(\varphi,\varphi')\right) \\ &\quad\cdot L^{M}_{\ell}\mathrm{U}(\pi-\varphi'), \qquad (11d)\end{aligned}$$

where the transition functions $F((\omega/c)X_{\ell})$, $L^{E,M}_{\ell}$ and $b_{\ell}(\varphi,\varphi')$ are given by

$$\begin{aligned} F((\omega/c)X_{\ell}) &= 2\sqrt{jX_{\ell}}e^{j(\omega/c)X_{\ell}}\int_{\sqrt{(\omega/c)X_{\ell}}}^{\infty}\exp(-j\tau^2)d\tau \\ &= \sqrt{\pi X_{\ell}}e^{j(\omega/c)X_{\ell}}erfc\left(\sqrt{j(\omega/c)X_{\ell}}\right), \qquad (12a)\end{aligned}$$

$$L^{E,M}_{1}=\cot\left[\frac{\pi-(\varphi-\varphi')}{2}\right] \quad \text{and} \quad L^{E,M}_{2}=\mp\cot\left[\frac{\pi-(\varphi+\varphi')}{2}\right], \tag{12b}$$

$$b_1(\varphi,\varphi')=2\cos^2\left(\frac{\varphi-\varphi'}{2}\right) \quad \text{and} \quad b_2(\varphi,\varphi')=2\cos^2\left(\frac{\varphi+\varphi'}{2}\right). \tag{12c}$$

The quantities $L_1^{E,M}$, $L_2^{E,M}$, b_1 and b_2 represent the discontinuous terms at the incident and reflected shadow boundaries for incidence from the upper side of the semi-lit half plane. It should be noted that the transition function used in [3] is equal to the one used by Kouyoumjian and Pathak [5]. Therefore, the transition function used in Refs. [3] and [5] corresponds to $\sqrt{j(\omega/c)}F((\omega/c)X_\ell)$ when using the expression given in Eq. (12a).

Similarly, the elements of the diffraction dyadic are equal to [3]

$$S^d_{\beta\beta'}(\varphi,\varphi',\beta;\omega) = \frac{\sqrt{j(\omega/c)}}{2n}\sum_{\ell=1}^{4} F\left((\omega/c)|\vec{R}-\vec{R}_e|\sin^2\beta a_\ell(\varphi,\varphi')\right)K_\ell^E, \tag{13a}$$

$$S^d_{\beta\varphi'} = 0, \tag{13b}$$

$$S^d_{\varphi\beta'} = 0, \tag{13c}$$

$$S^d_{\varphi\varphi'}(\varphi,\varphi',\beta;\omega) = \frac{\sqrt{j(\omega/c)}}{2n}\sum_{\ell=1}^{4} F\left((\omega/c)|\vec{R}-\vec{R}_e|\sin^2\beta a_\ell(\varphi,\varphi')\right)K_\ell^M, \tag{13d}$$

where $F((\omega/c)X_\ell)$ is defined in Eq. (12a) and

$$\begin{aligned} K_1^{E,M} &= \cot\left[\frac{\pi+(\varphi-\varphi')}{2n}\right] \quad \text{and} \quad K_2^{E,M} = \cot\left[\frac{\pi-(\varphi-\varphi')}{2n}\right], \\ K_3^{E,M} &= \mp\cot\left[\frac{\pi+(\varphi+\varphi')}{2n}\right] \quad \text{and} \quad K_4^{E,M} = \mp\cot\left[\frac{\pi-(\varphi+\varphi')}{2n}\right]. \end{aligned} \tag{14}$$

Here, $n\pi$ is the wedge angle as shown in Fig. 1. The functions $a_\ell(\varphi-\varphi')$ are given by

$$\begin{aligned} a_1(\varphi,\varphi') &= a^+(\varphi-\varphi'), \qquad a_2(\varphi,\varphi') = a^-(\varphi-\varphi'), \\ a_3(\varphi,\varphi') &= a^+(\varphi+\varphi'), \qquad a_4(\varphi,\varphi') = a^-(\varphi+\varphi'), \end{aligned} \tag{15a}$$

where

$$a^\pm(X) = 2\cos^2\left(\frac{2n\pi N^\pm - X}{2}\right). \tag{15b}$$

The quantities $N^\pm$ are the integer values that nearly satisfy the conditions

$$2n\pi N^\pm - X \approx \pm\pi. \tag{15c}$$

Combining Eqs. (9a,b) with (B7a,b) the dyadic-vector multiplications $\vec{\vec{S}}^{\,PO}_{SBL}(\vec{R}_{SBL})\cdot\vec{e}_i$ and $\vec{\vec{S}}^{\,d}(\vec{R}_e)\cdot\vec{e}_i$ can be evaluated to obtain the

shadow-boundary-line and the diffracted fields in the general Cartesian coordinates due to an incident field expressed in the general Cartesian coordinates at any edge point.

3.3. Time Domain Formulation of the Incremental Theory of Diffraction

Considering Eqs. (6), (7) and (8b), the time domain physical optics part due to an elementary point on the scattering surface can be calculated by applying the analytic inverse Fourier transformation of the frequency domain response. Specifically,

$$\begin{aligned}\vec{F}_s^{PO}(\vec{R},\vec{R}_s,t) &= \frac{-2\mathrm{U}((\pi/2)-\Theta')}{4\pi^2|\vec{R}-\vec{R}_s|}\vec{\vec{S}}_s^{PO}(\vec{R}_s)\\ &\quad\cdot\vec{e}_i\,\mathrm{Re}\left\{\int_0^\infty d\omega\left(j(\omega/c)E_i(\vec{R}_s,\omega)e^{-j\omega|\vec{R}-\vec{R}_s|/c}\right)e^{j\omega t}\right\}\\ &= \frac{-\mathrm{U}((\pi/2)-\Theta')}{2\pi^2|\vec{R}-\vec{R}_s|}\vec{\vec{S}}_s^{PO}(\vec{R}_s)\\ &\quad\cdot\vec{e}_i\,\mathrm{Re}\left\{\frac{j}{\left(a_0-j\left(ct-|\vec{R}-\vec{R}_s|-(\vec{R}_s-\vec{R}_0)\cdot\vec{s}_i\right)\right)^2}\right\}.\end{aligned}$$

The physical optics time domain part expressed explicitly in terms of the general Cartesian coordinates acquires the form

$$\begin{aligned}\vec{F}_s^{PO}(\vec{R},\vec{R}_s,t) &= \frac{-\mathrm{U}((\pi/2)-\Theta')}{2\pi^2|\vec{R}-\vec{R}_s|}\Pi^{-1}[\mathrm{P}_2(\Theta,\Phi)]\\ &\quad\cdot\begin{bmatrix}\cos\Theta\cos(\Phi-\Phi') & \cos\Theta\cos\Theta'\sin(\Phi-\Phi')\\ -\sin(\Phi-\Phi') & \cos\Theta'\cos(\Phi-\Phi')\end{bmatrix}\begin{bmatrix}e_\Theta^i\\ e_\Phi^i\end{bmatrix}\\ &\quad\times\mathrm{Re}\left\{\frac{j}{\left(a_0-j\left(ct-|\vec{R}-\vec{R}_s|-(\vec{R}_s-\vec{R}_0)\cdot\vec{s}_i\right)\right)^2}\right\}.\end{aligned}\tag{16}$$

where Eq. (A7) has been used to relate the local spherical coordinates to the general Cartesian ones.

Along the same vein, we need to convert the shadow-boundary-line field and diffracted field from the frequency domain to the time domain by evaluating the analytic inverse Fourier transformation of

the frequency domain response, viz.,

$$\vec{F}^{PO}_{SBL}(\vec{R},\vec{R}_{SBL},t) = \frac{1}{2\pi^2|\vec{R}-\vec{R}_{SBL}|}\mathrm{Re}\left[\int_0^\infty d\omega \vec{\vec{S}}^{\,PO}_{SBL}(\vec{R},\vec{R}_{SBL},\omega) \cdot\vec{e}_i e^{-(\omega/c)\left[a_0-j\left(ct-(\vec{R}_{SBL}-\vec{R}_0)\cdot\vec{s}_i-|\vec{R}-\vec{R}_{SBL}|\right)\right]}\right] \quad (17)$$

and

$$\vec{F}^{d}(\vec{R},\vec{R}_e,t) = \frac{1}{2\pi^2|\vec{R}-\vec{R}_e|}\mathrm{Re}\left[\int_0^\infty d\omega \vec{\vec{S}}^{\,d}(\vec{R},\vec{R}_e,\omega) \cdot\vec{e}_i e^{-(\omega/c)\left[a_0-j\left(ct-(\vec{R}_e-\vec{R}_0)\cdot\vec{s}_i-|\vec{R}-\vec{R}_e|\right)\right]}\right]. \quad (18)$$

It should be noted that, unlike the scattering dyadic of the physical optics part, both the shadow-boundary-line and the diffraction dyadics are frequency dependent. Therefore, these dyadics should be included in the kernels of the inverse Fourier transform integrations, as given by Eqs. (17) and (18).

Substituting Eqs. (10), (11) and (13) into Eqs. (17)–(18), it can be shown that the inverse Fourier transform leads to the expressions

$$\vec{F}^{PO}_{SBL}(\vec{R},\vec{R}_{SBL},t) = \frac{1}{2\pi^2|\vec{R}-\vec{R}_{SBL}|}\,\mathrm{II}^{-1}\left[\mathrm{P}_2(\beta,\varphi)\right] \cdot\begin{bmatrix} \Sigma^{SBL}_{\beta\beta'}(\vec{R},\vec{R}_{SBL},t) & \Sigma^{SBL}_{\beta\varphi'}(\vec{R},\vec{R}_{SBL},t) \\ \Sigma^{SBL}_{\varphi\beta'}(\vec{R},\vec{R}_{SBL},t) & \Sigma^{SBL}_{\varphi\varphi'}(\vec{R},\vec{R}_{SBL},t) \end{bmatrix}\begin{bmatrix} e^i_\beta \\ e^i_\varphi \end{bmatrix} \quad (19a)$$

and

$$\vec{F}^{d}(\vec{R},\vec{R}_e,t) = \frac{1}{2\pi^2|\vec{R}-\vec{R}_e|}\,\mathrm{II}^{-1}\left[\mathrm{P}_2(\beta,\varphi)\right] \cdot\begin{bmatrix} \Xi^{d}_{\beta\beta'}(\vec{R},\vec{R}_e,t) & \Xi^{d}_{\beta\varphi'}(\vec{R},\vec{R}_e,t) \\ \Xi^{d}_{\varphi\beta'}(\vec{R},\vec{R}_e,t) & \Xi^{d}_{\varphi\varphi'}(\vec{R},\vec{R}_e,t) \end{bmatrix}\begin{bmatrix} e^i_\beta \\ e^i_\varphi \end{bmatrix} \quad (19b)$$

where,

$$\Sigma^{SBL}_{\beta\beta'} = \sum_{\ell=1}^{2}\mathrm{Re}\left[I_2(\vec{R},t;X^{SBL}_\ell)\right]L^E_\ell \mathrm{U}(\pi-\varphi'), \quad (20a)$$

$$\Sigma^{SBL}_{\beta\varphi'} = -\mathrm{U}(\pi-\varphi')\mathrm{Re}\left[I_1(\vec{R},t)\right]\cos\beta, \quad (20b)$$

$$\Sigma^{SBL}_{\varphi\beta'} = 0, \quad (20c)$$

$$\Sigma^{SBL}_{\varphi\varphi'} \;=\; \sum_{\ell=1}^{2} \mathrm{Re}\left[I_2(\vec{R},t;X^{SBL}_{\ell})\right] L^{M}_{\ell}\mathrm{U}(\pi-\varphi'), \tag{20d}$$

and

$$\Xi^{d}_{\beta\beta'} \;=\; (1/n)\sum_{\ell=1}^{4} \mathrm{Re}\left[I_2(\vec{R},t;X^{e}_{\ell})\right] K^{E}_{\ell}, \tag{21a}$$

$$\Xi^{d}_{\beta\varphi'} \;=\; 0, \tag{21b}$$

$$\Xi^{d}_{\varphi\beta'} \;=\; 0, \tag{21c}$$

$$\Xi^{d}_{\varphi\varphi'} \;=\; (1/n)\sum_{\ell=1}^{4} \mathrm{Re}\left[I_2(\vec{R},t;X^{e}_{\ell})\right] K^{M}_{\ell}. \tag{21d}$$

In the above expressions, the integrations $I_1(\vec{R},t)$ and $I_2(\vec{R},t;X^{*}_{\ell})$ are evaluated as follows:

$$I_1(\vec{R},t)=\int_0^{\infty} d\omega \exp\Big(-\omega\left\{a_0-j\left(ct-(\vec{R}_{SBL}-\vec{R}_0)\cdot\vec{s}_i-|\vec{R}-\vec{R}_{SBL}|\right)\right\}/c\Big)$$

$$=\frac{1}{\left\{a_0-j\left(ct-(\vec{R}_{SBL}-\vec{R}_0)\cdot\vec{s}_i-|\vec{R}-\vec{R}_{SBL}|\right)\right\}/c}, \tag{22}$$

$$I_2(\vec{R},t;X^{*}_{\ell}) \;=\; \frac{1}{2}\int_0^{\infty} d\omega\sqrt{j(\omega/c)}F\left((\omega/c)|\vec{R}-\vec{R}^{*}|\alpha_{\ell}(\varphi,\varphi')\sin^2\beta\right)$$

$$\cdot\, e^{-(\omega/c)\left(a_0-j\left(ct-(\vec{R}^{*}-\vec{R}_0)\cdot\vec{s}_i-|\vec{R}-\vec{R}^{*}|\right)\right)}. \tag{23}$$

In the latter expression, $\alpha_{\ell}(\varphi,\varphi')$ denotes either $a_{\ell}(\varphi,\varphi')$ or $b_{\ell}(\varphi,\varphi')$, while the asterisk in $\vec{R}^{*}$ and X^{*}_{ℓ} refers to either the edge or the shadow-boundary-line. Using the definition of the transition function $F((\omega/c)X_{\ell})$ given in Eq. (12a), the above integration can be rewritten as

$$I_2(\vec{R},t;X^{*}_{\ell}) \;=\; \frac{1}{2}\sqrt{\pi q(\vec{R})}\int_0^{\infty} d\omega\sqrt{\omega}\exp\left(-\omega\left(p(t,\vec{R})-q(\vec{R})\right)\right)$$

$$erfc\left(\sqrt{\omega q(\vec{R})}\right), \tag{24a}$$

where

$$p(t,\vec{R}) \;=\; -(j/c)\left(ja_0+\left(ct-(\vec{R}^{*}-\vec{R}_0)\cdot\vec{s}_i-|\vec{R}-\vec{R}^{*}|\right)\right), \tag{24b}$$

$$q(\vec{R}) \;=\; j\left[|\vec{R}-\vec{R}^{*}|\sin^2\beta\alpha_{\ell}(\varphi,\varphi')\right]/c. \tag{24c}$$

The integration in Eq. (21) can be carried out using of the identity (6.292) in Ref. [19]. Defining the variable $N(t,\vec{R}) = (p(t,\vec{R}) - q(\vec{R}))/q(\vec{R})$, we obtain explicitly

$$\int_0^\infty \sqrt{\omega} erfc\,(\sqrt{\omega q}) \exp[-Nq\omega] d\omega = \frac{1}{q^{3/2}\sqrt{\pi}} \left[\frac{\tan^{-1}\sqrt{N}}{(N)^{3/2}} - \frac{1}{(N)(N+1)} \right], \tag{25}$$

where $|\arg(\sqrt{N})| < \pi/4$. Now Eq. (25) can be used to evaluate the integration in Eq. (21). For $a_0 > 0$, thus $\mathrm{Re}(p(t,\vec{R})) > 0$, whereas, $q(\vec{R})$ is purely imaginary. Consequently, the argument of the function $(p(t,\vec{R}) - q(\vec{R}))$ for time larger than or equal the arrival time of the wave front, $t \geq ((\vec{R}^* - \vec{R}_0)\cdot\vec{s}_i + |\vec{R} - \vec{R}^*|)/c$, is $0 < \arg(p-q) < \pi/2$, and the argument of the function $q(\vec{R})$ is $\arg(q(\vec{R})) = \pi/2$. Thus, the absolute value of argument of $\sqrt{N}$ has the property $|\arg(\sqrt{N})| < \pi/4$, which satisfies the condition of validity of Eq. (25). Consequently, the integration given in Eq. (21) reduces to

$$I_2(\vec{R},t;X_\ell^*) = \frac{1}{2q(\vec{R})} \left[\frac{\tan^{-1}\sqrt{N(t,\vec{R})}}{(N(t,\vec{R}))^{3/2}} - \frac{1}{N(t,\vec{R})(N(t,\vec{R})+1)} \right], \tag{26}$$

for $t \geq ((\vec{R}^* - \vec{R}_0)\cdot\vec{s}_i + (\vec{R} - \vec{R}^*))/c$. Substituting Eqs. (22) and Eq. (26) in Eqs. (19)–(21), one obtains the time-domain shadow-boundary-line and the time domain diffracted elementary amplitudes of the scattered field, respectively. The total time-domain field can be obtained by combining these two parts with the physical optics part, given in Eq. (16). The total scattered field is then calculated after carrying out the following integrations:

$$\begin{aligned} \vec{E}_s^{tot}(\vec{R},t) \;=\; & \iint_S \vec{F}_s^{PO}(\vec{R},\vec{R}_s,t) dS - \int_{SBL} \vec{F}_{SBL}^{PO}(\vec{R},\vec{R}_{SBL},t) dl \\ & + \int_e \vec{F}^d(\vec{R},\vec{R}_e,t) dl. \end{aligned} \tag{27}$$

4. TD-ITD RESULTS FOR THE DIFFRACTION OF A PULSED PLANE WAVE NORMALLY INCIDENT ON A PERFECTLY CONDUCTING CIRCULAR DISK

In this section, the total field in the back-scattering region of a perfectly conducting circular disk due to a normally incident pulsed

plane wave is calculated using the TD-ITD method. We are primarily interested in the backscattered fields, which can be used for detection and identification of the scattering object. The forward scattered field is mainly affected by the diffraction part of the shadow boundary line rather than by the current distribution on the illuminated part of the scattering surface. In principle, we can calculate the forward-scattered part; however this is not done just to simplify the numerical computations. TD-ITD has been used to calculate the total field in the back-scattering region due to a pulsed plane wave normally incident on a perfectly conducting circular disk of radius $L = 50\,\text{cm}$. In Fig. 4, we display the y-component of the total field in the back-scattering region. The incident field has a spectrum $E(\omega) = \exp(-a_0\omega/c)$, $a_0 = 3\,\text{cm}$. A reference point on the pulsed plane wave at $t = 0$ is $(x_0, y_0, z_0) = (0, 0, 110\,\text{cm})$. The incident pulsed plane wave has a y-polarization and the y component of the total field is plotted in the xz plane at $t = 5$ and 8 ns. The total field is normalized with respect to the peak value of the incident pulsed plane wave and is plotted using a sixteen-level gray-scale. Fig. 4a shows that behind the main reflected wavefront, there are additional spherical wavefronts having the same radius and center as the diffraction wavefronts. Such secondary spherical wavefronts do not appear in the TD-UTD solution [6, 20]. They are a combination of the diffracted fields and the physical optics fields that are truncated by the finiteness of the size of the disk. The spatial separation between the original pulse and the image along the axis of the disk is equal to the difference between the two path lengths measured from the center of the disk and from its edge. For $t = 5\,\text{ns}$, the total path traveled by the wavefront along the axis of the disk is 150 cm. Since the initial wavefront is located at $z = 110$, the main reflected wave front is located on the axis of the disk at $z = 40$. The path from the edge of the disk to the center of the wavefront along the axis of the disk is nearly 64 cm. The difference between the two path lengths from the center of the disk and from its edge to the center of the reflected wavefront is mirrored by the spatial distance between the original pulse and the secondary wavefront. In Fig. 4a, the trailing wavefront is significantly delayed after the main reflected pulse because the observation distance is small. In this case, the difference between these two paths is nearly 24 cm. On the other hand, this difference decreases to 9.2 cm for $t = 8\,\text{ns}$. Fig. 4b illustrates how the separation between the main reflected pulse and the trailing wavefront shrinks at farther distances.

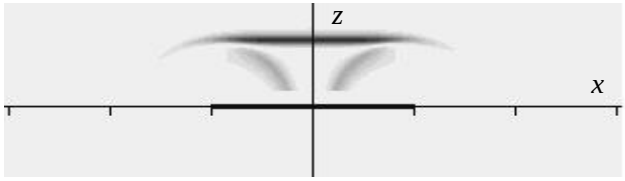

(a) $t = 5$ ns

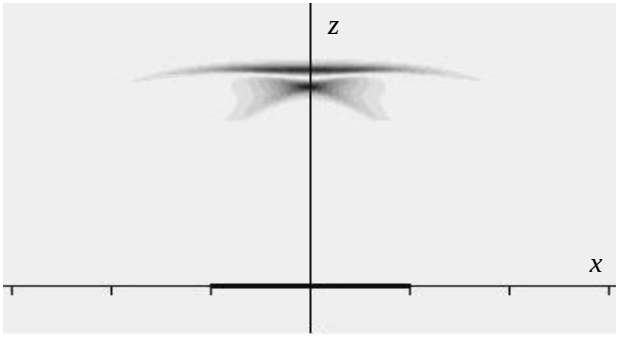

(b) $t = 8$ ns

Figure 4. Total y-component of the backscattered field due to a pulsed plane wave normally incident on a perfectly conducting circular disk of radius $L = 50\,\text{cm}$. The incident field has a spectrum $E(\omega) = \exp(-a_0\omega/c)$, $a_0 = 3\,\text{cm}$. A reference point on the pulsed plane wave at $t = 0$ is $(x_0, y_0, z_0) = (0, 0, 110\,\text{cm})$.

5. CONCLUDING REMARKS

In an earlier study of the scattering of an TE X-wave pulse from a circular disk, an approach based on the time-domain uniform theory of diffraction (TD-UTD) was used [21]. However, the derived TD-UTD solutions of the disk problem had some drawbacks, namely, the existence of field singularities at the caustics and the limitation of the diffracted fields to the Keller's diffraction cone [22]. The diffraction cones are based on the presence of infinite edges. In addition, the geometrical optics component of the field depends only on the presence of a specular point and is independent of the distance between the scattering structure and the observation point. This is a serious drawback when dealing with a finite structure. These disadvantages have motivated us to formulate a TD-ITD approach for solving the problem of diffraction of a pulse plane wave by a perfectly conducting circular disk. The evaluated scattered field is shown to be free of

singularities. In Ref. [18], the approach developed in this paper is applied to the scattering of an electromagnetic X-wave from a circular disk.

APPENDIX A.

A general three-dimensional scattering surface can be represented in Cartesian coordinates by the position vector [7],

$$\vec{R}_s(u,v) = x_s(u,v)\vec{a}_x + y_s(u,v)\vec{a}_y + z_s(u,v)\vec{a}_z. \tag{A1}$$

where u and v are two independent parametric variables. For the case of a circular disk, the scattering surface can be represented as

$$\vec{R}_s(u,v) = R\sin u\cos v\vec{a}_x + R\sin u\sin v\vec{a}_y, \tag{A2}$$

where $0 \le u \le \pi/2$ and $0 \le v \le 2\pi$. The local X and Y directions can be obtained as follows:

$$\vec{a}_X = \vec{R}_{su}(u,v)/|\vec{R}_{su}(u,v)|, \tag{A3a}$$

$$\vec{a}_Y = \vec{R}_{sv}(u,v)/|\vec{R}_{sv}(u,v)|. \tag{A3b}$$

Here, $\vec{R}_{su}(u,v) = \partial\vec{R}_s(u,v)/\partial u$, and $\vec{R}_{sv}(u,v) = \partial\vec{R}_s(u,v)/\partial v$. The local Z direction at the scattering point is the normal direction to the scattering surface at this point, namely,

$$\vec{a}_Z = \vec{n}(u,v) = \frac{\vec{R}_{su}\times\vec{R}_{sv}}{|\vec{R}_{su}\times\vec{R}_{sv}|}. \tag{A3c}$$

Eq. (A3) represents a simple relation between the local Cartesian coordinates at the scattering point and the general Cartesian coordinates. Such a relation can be formulated in a dyadic form as follows:

$$\begin{bmatrix} \vec{a}_X \\ \vec{a}_Y \\ \vec{a}_Z \end{bmatrix} = \Pi \begin{bmatrix} \vec{a}_x \\ \vec{a}_y \\ \vec{a}_z \end{bmatrix} = \begin{bmatrix} \cos v & \sin v & 0 \\ -\sin v & \cos v & 0 \\ 0 & 0 & 1 \end{bmatrix} \begin{bmatrix} \vec{a}_x \\ \vec{a}_y \\ \vec{a}_z \end{bmatrix}. \tag{A4}$$

The local spherical angles (Θ', Φ') and (Θ, Φ) of the incident and scattered fields can be expressed as

$$\Theta' = \cos^{-1}\left[-\vec{s}_i, \vec{a}_Z\right], \tag{A5a}$$

$$\Phi' = \pi - \mathrm{sgn}\left(-\vec{s}_i\cdot\vec{a}_Y\right)\left\{\pi - \cos^{-1}\left(-\vec{s}_i\cdot\vec{a}_X/\sin\Theta'\right)\right\}, \tag{A5b}$$

$$\Theta = \cos^{-1}\left((\vec{R}-\vec{R}_s)\cdot\vec{a}_Z/|\vec{R}-\vec{R}_s|\right), \tag{A5c}$$

$$\Phi = \pi - \mathrm{sgn}\left((\vec{R}-\vec{R}_s)\cdot\vec{a}_Y\right) \cdot\left\{\pi - \cos^{-1}\left((\vec{R}-\vec{R}_s)\cdot\vec{a}_X/\left(|\vec{R}-\vec{R}_s|\sin\Theta\right)\right)\right\}. \tag{A5d}$$

The scattering dyadic is given in the local spherical coordinates for both the incident and the scattered rays. Thus, to evaluate the vector product $\vec{\vec{S}}_s^{PO}(\vec{R}_s) \cdot \vec{e}_i$ in Eq. (8a), the components of the polarization vector of the incident wave should be transformed from the general Cartesian coordinates to the local spherical coordinates. Using the transformation matrix Π, we write the required transformation as

$$\begin{bmatrix} e_\Theta^i \\ e_\Phi^i \end{bmatrix} = [\mathrm{P}_1(\Theta', \Phi')]\Pi \begin{bmatrix} e_x^i \\ e_y^i \\ e_z^i \end{bmatrix}, \tag{A6a}$$

where

$$[\mathrm{P}_1(\Theta', \Phi')] = \begin{bmatrix} \cos\Theta'\cos\Phi' & \cos\Theta'\sin\Phi' & -\sin\Theta' \\ -\sin\Phi' & \cos\Phi' & 0 \end{bmatrix}. \tag{A6b}$$

The components of the scattered field that are obtained from the dyadic-vector multiplication $\vec{\vec{S}}_s^{PO}(\vec{R}_s) \cdot \vec{e}_i$ are expressed in the local Θ and Φ spherical directions. These components of the scattered field can be converted to the general Cartesian coordinates, viz.,

$$\begin{bmatrix} e_x^s \\ e_y^s \\ e_z^s \end{bmatrix} = \Pi^{-1}[\mathrm{P}_2(\Theta, \Phi)] \begin{bmatrix} e_\Theta^s \\ e_\Phi^s \end{bmatrix} = \Pi^{-1}[\mathrm{P}_2(\Theta, \Phi)] \left[\vec{\vec{S}}_s^{PO}(\vec{R}_s)\right] \begin{bmatrix} e_\Theta^i \\ e_\Phi^i \end{bmatrix}, \tag{A7a}$$

where $\left[\vec{\vec{S}}_s^{PO}(\vec{R}_s)\right]$ is the 2×2 matrix representation of the dyadic given in Eq. (8b) and

$$[\mathrm{P}_2(\Theta, \Phi)] = \begin{bmatrix} \cos\Theta\cos\Phi & -\sin\Phi \\ \cos\Theta\sin\Phi & \cos\Phi \\ -\sin\Theta & 0 \end{bmatrix}. \tag{A7b}$$

APPENDIX B.

In Eqs. (11)–(13), the angles φ', φ, and β are the spherical angles specifying the incident and the diffracted rays at the edge diffraction point as shown in Figs. 1 and 3. At the edge points, the local Z direction is chosen tangential to the edge. The local X direction is assumed to be the normal to the edge at the same point and tangential to the upper surface of the local wedge. To obtain these directions, the location of a general point along either the edge or the shadow boundary can be expressed as a function of a single parametric variable

γ. In what follows, an edge point is expressed by the following position vector [7]

$$\vec{R}_e(\gamma) = x(\gamma)\vec{a}_x + y(\gamma)\vec{a}_y + z(\gamma)\vec{a}_z. \tag{B1}$$

Thus, the tangential and the normal directions to the edge at any point along the edge are given by [7]

$$\vec{e}(\gamma) = \vec{a}_Z(\gamma) = (d\vec{R}(\gamma)/d\gamma)/|d\vec{R}(\gamma)/d\gamma|, \tag{B2a}$$
$$\vec{n}_p(\gamma) = \vec{a}_X(\gamma) = (d\vec{e}(\gamma)/d\gamma)/|d\vec{e}(\gamma)/d\gamma|. \tag{B2b}$$

From the above two directions, one can obtain the third local direction; specifically,

$$\vec{a}_Y = -\vec{a}_X \times \vec{a}_Z. \tag{B2c}$$

For the case of a circular disk, the parametric representation of its edge can be written as

$$\vec{R}_e(\gamma) = R\cos\gamma\vec{a}_x + R\sin\gamma\vec{a}_y, \tag{B3a}$$
$$\vec{e}(\gamma) = \vec{a}_Z(\gamma) = -\sin\gamma\vec{a}_x + \cos\gamma\vec{a}_y, \tag{B3b}$$
$$\vec{n}_p(\gamma) = \vec{a}_X(\gamma) = -\cos\gamma\vec{a}_x - \sin\gamma\vec{a}_y, \tag{B3c}$$
$$\vec{a}_Y = \vec{a}_z. \tag{B3d}$$

Using Eq. (B3), the relation between the local Cartesian coordinates and the general Cartesian coordinates can be expressed in terms of the matrix transformation

$$\begin{bmatrix} \vec{a}_X \\ \vec{a}_Y \\ \vec{a}_Z \end{bmatrix} = \amalg \begin{bmatrix} \vec{a}_x \\ \vec{a}_y \\ \vec{a}_z \end{bmatrix} = \begin{bmatrix} -\cos\gamma & -\sin\gamma & 0 \\ 0 & 0 & 1 \\ -\sin\gamma & \cos\gamma & 0 \end{bmatrix} \begin{bmatrix} \vec{a}_x \\ \vec{a}_y \\ \vec{a}_z \end{bmatrix}. \tag{B4}$$

Due to the similarity between the problem of the edge and the problem of the shadow boundary line, the following analysis is presented in terms of the edge parameters and can be applied directly to the shadow boundary line parameters by exchanging $\vec{R}_e$ by $\vec{R}_{SBL}$. The spherical angles of the incident and diffracted rays in the local spherical coordinates can now be obtained in terms of the local Cartesian coordinates; specifically,

$$\beta = \cos^{-1}\left\{(\vec{R} - \vec{R}_e)\cdot\vec{a}_Z/|\vec{R} - \vec{R}_e|\right\}, \tag{B5a}$$
$$\varphi = \pi - \mathrm{sgn}\Big((\vec{R} - \vec{R}_e)\cdot\vec{a}_Y\Big)\Big(\pi - \cos^{-1}\Big\{(\vec{R} - \vec{R}_e)\cdot\vec{a}_X/|\vec{R} - \vec{R}_e|\sin\beta_0\Big\}\Big), \tag{B5b}$$
$$\beta' = \cos^{-1}\left\{-\vec{s}_i\cdot\vec{a}_Z\right\}, \tag{B5c}$$
$$\varphi' = \pi - \mathrm{sgn}\left(-\vec{s}_i\cdot\vec{a}_Y\right)\left(\pi - \cos^{-1}\left\{-\vec{s}_i\cdot\vec{a}_X/\sin\beta'\right\}\right). \tag{B5d}$$

Both the physical optics end line dyadic and the diffraction dyadic are expressed in the local spherical coordinates for both the incident and the diffracted rays. Thus, to evaluate the vector products $\vec{\vec{S}}^{\,PO}_{SBL}(\vec{R}_{SBL}) \cdot e_i$ and $\vec{\vec{S}}^{\,d}(\vec{R}_e) \cdot e_i$ the components of the incident field should be transformed from the general Cartesian coordinates to the local spherical coordinates. Given the transformation dyadic II, which transforms from the general Cartesian coordinates to the local Cartesian coordinates of the edge, the transformation of the components of the incident field is given by

$$\begin{bmatrix} e^i_\beta \\ e^i_\varphi \end{bmatrix} = [\mathrm{P}_1(\beta', \varphi')]\, \mathrm{II} \begin{bmatrix} e^i_x \\ e^i_y \\ e^i_z \end{bmatrix}, \tag{B6a}$$

$$[P_1(\beta', \varphi')] = \begin{bmatrix} \cos\beta' \cos\varphi' & \cos\beta' \sin\varphi' & -\sin\beta' \\ -\sin\varphi' & \cos\varphi' & 0 \end{bmatrix}. \tag{B6b}$$

The field components of both the shadow boundary line fields and the diffracted fields are obtained from the dyadic-vector multiplications $\vec{\vec{S}}^{\,PO}_{SBL}(\vec{R}_{SBL}) \cdot \vec{e}_i$ and $\vec{\vec{S}}^{\,d}(\vec{R}_e) \cdot \vec{e}_i$. The results are expressed in the local β and φ spherical coordinates. Such field components can be converted to the general Cartesian coordinates as follows:

$$\begin{bmatrix} e^d_x \\ e^d_y \\ e^d_z \end{bmatrix} = \mathrm{II}^{-1}[P_2(\beta, \varphi)] \begin{bmatrix} e^d_\beta \\ e^d_\varphi \end{bmatrix} = \mathrm{II}^{-1}[P_2(\beta, \varphi)] \left[\vec{\vec{S}}^{\,d}_s(\vec{R}_e)\right] \begin{bmatrix} e^i_\beta \\ e^i_\varphi \end{bmatrix}. \tag{B7a}$$

Here,

$$[P_2(\beta, \varphi)] = \begin{bmatrix} \cos\beta\cos\varphi & -\sin\varphi \\ \cos\beta\sin\varphi & \cos\varphi \\ -\sin\beta & 0 \end{bmatrix}. \tag{B7b}$$

$\left[\vec{\vec{S}}^{\,d}_s(\vec{R}_e)\right]$ is the 2×2 matrix representation of the dyadic given in Eq. (10).

REFERENCES

1. Capolino, F. and R. Tiberio, "A time-domain incremental theory of diffraction (TD-ITD) for a wedge," *Proceedings of the International Conference on Electromagnetic in Advanced Application (ICEAA 01)*, Torino, Italy, September 10–14, 2001.

2. Tiberio, R. and S. Maci, "An incremental theory of diffraction: scalar formulation," *IEEE Trans. Antennas and Prop.*, Vol. 42, 600–611, 1994.
3. Tiberio, R., S. Maci, and A. Toccafondi, "An incremental theory of diffraction: electromagnetic formulation," *IEEE Trans. Antennas and Prop.*, Vol. 43, 87–96, 1995.
4. Maci, S., R. Tiberio, and A. Toccafondi, "Incremental diffraction coefficients for source and observation at finite distances from an edge," *IEEE Trans. Antennas and Prop.*, Vol. 44, 593–599, 1996.
5. Kouyoumjian, R. G. and P. H. Pathak, "A uniform geometrical theory of diffraction for an edge in a perfectly conducting surface," *Proc. IEEE*, Vol. 62, 1448–1461, 1974.
6. Rousseau, P. R. and P. H. Pathak, "Time-domain uniform geometrical theory of diffraction for a curved wedge," *IEEE Trans. Antennas and Prop.*, Vol. 43, 1375–1382, 1995.
7. McNamara, D. M., C. W. I. Pistorius, and J. A. G. Malherba, *Introduction to the Uniform Geometrical Theory of Diffraction*, Artech House, Boston, 1990.
8. Jones, D. S., *The Theory of Electromagnetism*, Pergamon, Oxford, 1964.
9. James, G. L., *Geometrical Theory of Diffraction for Electromagnetic Waves*, Peter Peregrinus, IEE, London, 1986.
10. Borovikov, V. A. and B. Ye. Kinber, *Geometrical Theory of Diffraction*, IEE, London, 1994.
11. Ryan, C. and L. Peters, "Evaluation of edge-diffracted fields including equivalent currents for the caustic regions," *IEEE Trans. Antennas and Prop.*, Vol. 17, 292–299, 1969.
12. Michaeli, A., "Equivalent edge currents for arbitrary aspects of observation," *IEEE Trans. Antennas and Prop.*, Vol. 32, 252–258, 1984.
13. Johansen, P., "Uniform physical theory of diffraction equivalent edge currents for truncated wedge strips," *IEEE Trans. Antennas and Prop.*, Vol. 44, 989–995, 1996.
14. Sun, E. and W. Rusch, "Time-domain physical optics," *IEEE Trans. Antennas and Prop.*, Vol. 42, 9–15, 1994.
15. Gupta, I. and W. Burnside, "A physical optics correction for backscattering from curved surfaces," *IEEE Trans. Antennas and Prop.*, Vol. 35, 553–561, 1987.
16. Gupta, I., C. Pistorious, and W. Burnside, "An efficient method to compute spurious end point contributions in PO solutions," *IEEE Trans. Antennas and Prop.*, Vol. 35, 1426–1435, 1987.

17. Johansen, P., "Time-domain version of the physical theory of diffraction," *IEEE Trans. Antennas and Prop.*, Vol. 47, 261–270, 1999.
18. Attiya, A. M., E. El-Diwany, A. M. Shaarawi, and I. M. Besieris, "Scattering of X-waves from a circular disk using a time domain incremental theory of diffraction," submitted to the same journal.
19. Gradshteyn, I. S. and I. M. Ryzhik, *Table of Integrals, Series and Products*, Fifth Edition, Academic Press, Boston, 1994.
20. Veruttipong, T. W., "Time-domain version of the uniform GTD," *IEEE Trans. Antennas and Prop.*, Vol. 38, 1757–1764, 1990.
21. Attiya, A. M., E. El-Diwany, A. M. Shaarawi, and I. M. Besieris, "Diffraction of a transverse electric (TE) X wave by conducting objects," Accepted for publication.
22. Keller, J. B., "Geometrical theory of diffraction," *J. Opt. Soc. Am.*, Vol. 52, 116–130, 1962.